

Electronic Supplementary Information for:

**Studies on the chemical reduction of polynuclear titanium(IV) nitrido
complexes**

Jorge Caballo, Adrián Calvo-Molina, Sergio Claramonte, Maider Greño, Adrián Pérez-Redondo and Carlos Yélamos*

Departamento de Química Orgánica y Química Inorgánica, Instituto de Investigación Química “Andrés M. del Río” (IQAR), Universidad de Alcalá, 28805 Alcalá de Henares-Madrid (Spain). E-mail: carlos.yelamos@uah.es

Contents:

- Cyclic voltammograms of complexes **1**, **3**, **4**, and **14**.
- Experimental crystallographic data of complexes **5**, **11**, **13**, and **17**.
- Perspective view of the crystal structure of compounds **5**, **11**, and **13**.
- Table for selected lengths and angles of the crystal structures of **5**, **11**, **13**, and **17**.
- EPR spectra for complex **7**.
- Selected ^1H and $^{13}\text{C}\{^1\text{H}\}$ NMR spectra.

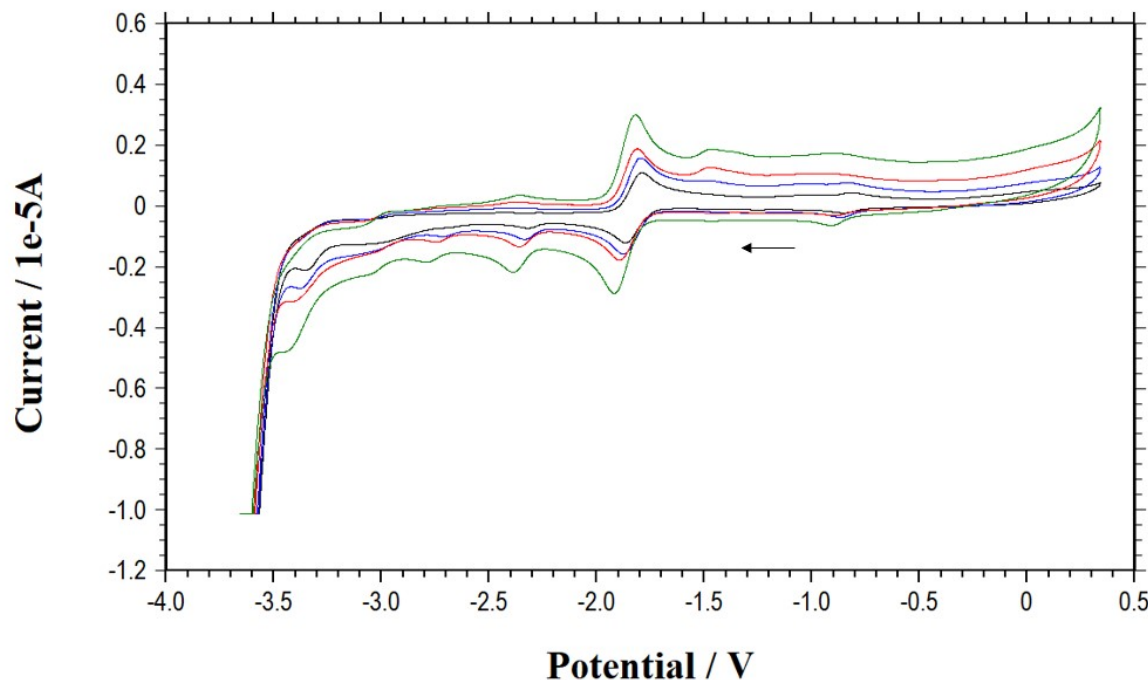


Figure S1. Cyclic voltammograms of $[\{\text{Ti}_4(\eta^5\text{-C}_5\text{Me}_5)_4\}(\mu_3\text{-N})_4]$ (**1**) in *thf*/0.1 M $[\text{N}(n\text{Bu})_4]\text{[PF}_6]$ versus Fc^+/Fc at 22 °C at 50 (black line), 100 (blue line), 200 (red line) and 500 (green line) mV s⁻¹ scan rate.

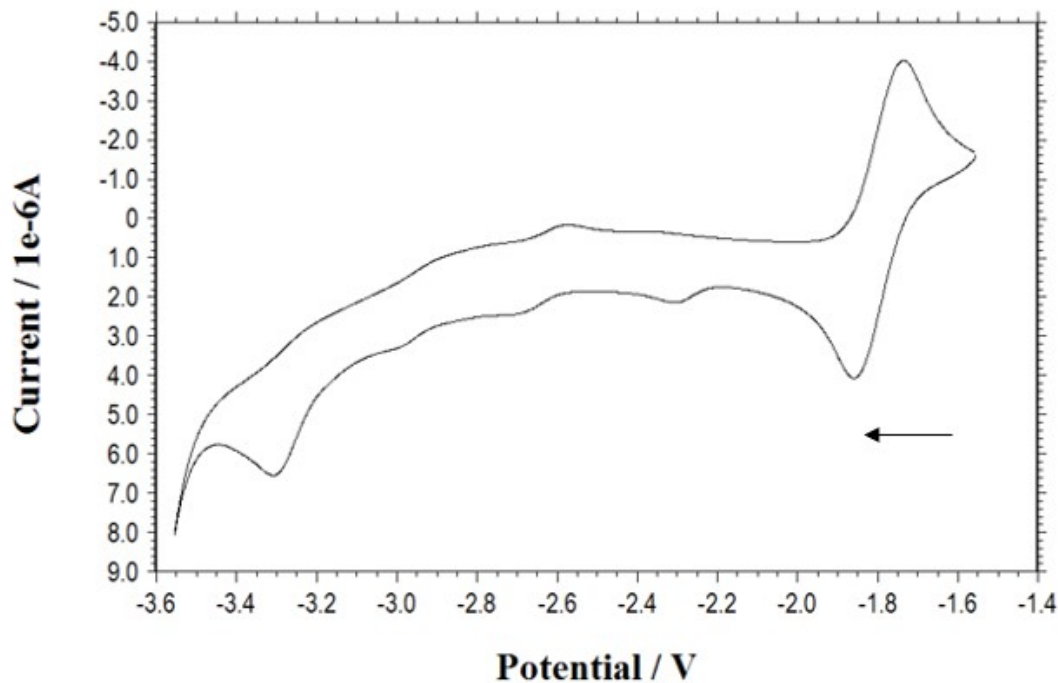


Figure S2. Cyclic voltammogram of $[\{\text{Ti}_4(\eta^5\text{-C}_5\text{Me}_5)_3(\eta^5\text{-C}_5\text{H}_4\text{SiMe}_3)\}(\mu_3\text{-N})_4]$ (**3**) in *thf*/0.1 M $[\text{N}(n\text{Bu})_4]\text{[PF}_6]$ versus Fc^+/Fc at 50 mV s⁻¹ scan rate at 22 °C.

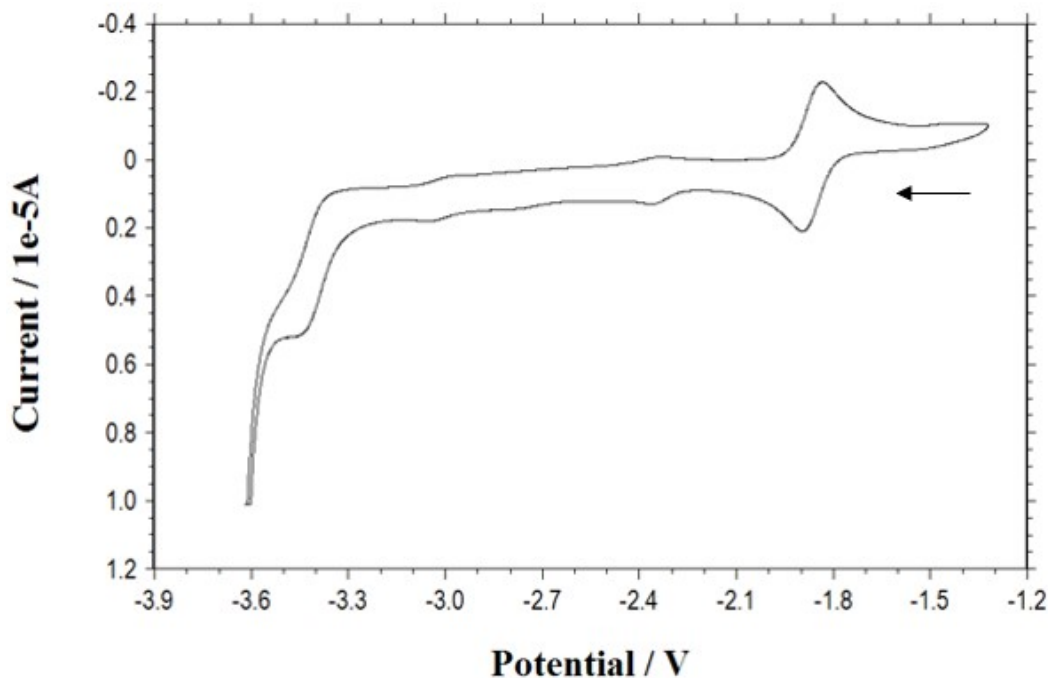


Figure S3. Cyclic voltammogram of $[\{\text{Ti}_4(\eta^5\text{-C}_5\text{Me}_5)_3(\eta^5\text{-C}_5\text{H}_5)\}(\mu_3\text{-N})_4]$ (**4**) in thf/0.1 M $[\text{N}(n\text{Bu})_4]\text{[PF}_6]$ versus Fc^+/Fc at 50 mV s^{-1} scan rate at 22°C .

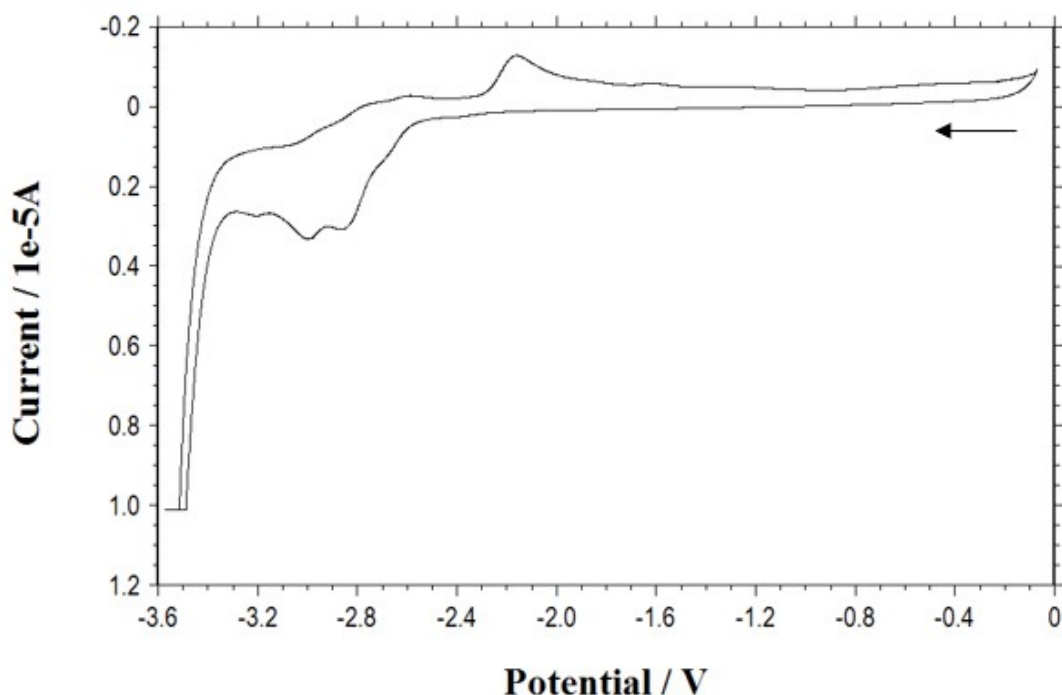


Figure S4. Cyclic voltammogram of $[\{\text{Ti}(\eta^5\text{-C}_5\text{Me}_5)(\mu\text{-NH})_3(\mu_3\text{-N})\}]$ (**14**) in thf/0.1 M $[\text{N}(n\text{Bu})_4]\text{[PF}_6]$ versus Fc^+/Fc at 50 mV s^{-1} scan rate at 22°C .

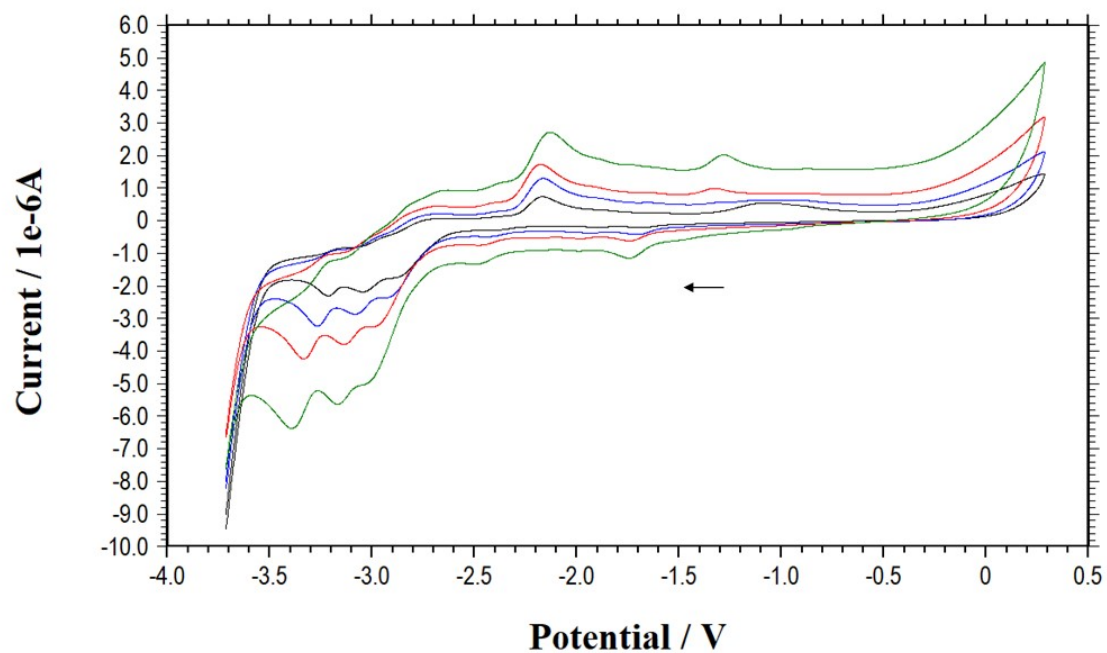


Figure S5. Cyclic voltammograms of $[\{\text{Ti}(\eta^5\text{-C}_5\text{Me}_5)(\mu\text{-NH})\}_3(\mu_3\text{-N})]$ (**14**) in thf/0.1 M $[\text{N}(n\text{Bu})_4]\text{[PF}_6]$ versus Fc^+/Fc at 22 °C at 50 (black line), 100 (blue line), 200 (red line) and 500 (green line) mV s $^{-1}$ scan rate.

Table S1. Experimental Data for the X-ray Diffraction Studies on **5**, **11**, **13**, and **17**.

	5	11·C₆H₆	13·2C₇H₈	17
Formula	C ₆₄ H ₁₀₈ N ₄ NaO ₆ Ti ₄	C ₆₂ H ₁₀₀ KN ₆ O ₆ SiTi ₄	C ₇₈ H ₁₁₉ K ₂ N ₄ O ₁₂ Ti ₄	C ₅₀ H ₇₁ KN ₄ O ₆ Ti ₃
M _r	1244.13	1284.26	1574.56	1006.9
T [K]	150(2)	150(2)	200(2)	150(2)
λ [Å]	0.71073	0.71073	0.71073	0.71073
crystal system	Cubic	Orthorhombic	Triclinic	Monoclinic
space group	<i>I</i> 2 ₁ 3	<i>P</i> 2 ₁ 2 ₁ 2	<i>P</i> -1	<i>P</i> 2 ₁ /c
<i>a</i> [Å]; α [°]	23.803(5)	23.739(3)	11.661(1); 85.26(1)	18.208(1)
<i>b</i> [Å]; β [°]		33.351(3)	18.772(1); 78.97(1)	12.389(2); 102.42(1)
<i>c</i> [Å]; γ [°]		16.799(3)	20.043(2); 81.01(1)	22.664(2)
<i>V</i> [Å ³]	13487(9)	13300(3)	4247.0(6)	4992.9(9)
Z	8	8	2	4
ρ _{calcd} [g cm ⁻³]	1.225	1.283	1.231	1.340
μ _{MoKα} [mm ⁻¹]	0.512	0.595	0.517	0.603
<i>F</i> (000)	5336	5464	1674	2128
crystal size [mm ³]	0.27 × 0.24 × 0.19	0.18 × 0.17 × 0.16	0.40 × 0.27 × 0.14	0.37 × 0.35 × 0.35
θ range [deg]	2.71 to 27.58	3.03 to 23.30	3.04 to 25.24	3.09 to 27.50
index ranges	-30 to 31, -31 to 31, -31 to 31	-26 to 26, -28 to 37, -18 to 18	-13 to 13, -22 to 22, -24 to 24	-23 to 23, -16 to 16, -29 to 29
Reflections collected	208791	111322	79483	92796
Unique data	5225 [<i>R</i> (int) = 0.101]	19134 [<i>R</i> (int) = 0.080]	15316 [<i>R</i> (int) = 0.100]	11448 [<i>R</i> (int) = 0.103]
obsd data [<i>I</i> >2σ(<i>I</i>)]	4592	13416	10174	7266
Goodness-of-fit on F ²	1.088	1.016	1.057	1.097
final R ^a indices [<i>I</i> >2σ(<i>I</i>)]	R1 = 0.045, wR2 = 0.097	R1 = 0.057, wR2 = 0.106	R1 = 0.062, wR2 = 0.145	R1 = 0.055, wR2 = 0.101
R ^a indices (all data)	R1 = 0.058, wR2 = 0.108	R1 = 0.098, wR2 = 0.118	R1 = 0.102, wR2 = 0.175	R1 = 0.117, wR2 = 0.130
largest diff. peak/hole [e Å ⁻³]	0.614 and -0.328	0.387 and -0.300	0.528 and -0.466	0.519 and -0.428

$$^a RI = \sum |F_0| - |F_c| / [\sum |F_0|] \quad wR2 = \{[\sum w(F_0^2 - F_c^2)^2] / [\sum w(F_0^2)^2]\}^{1/2}$$

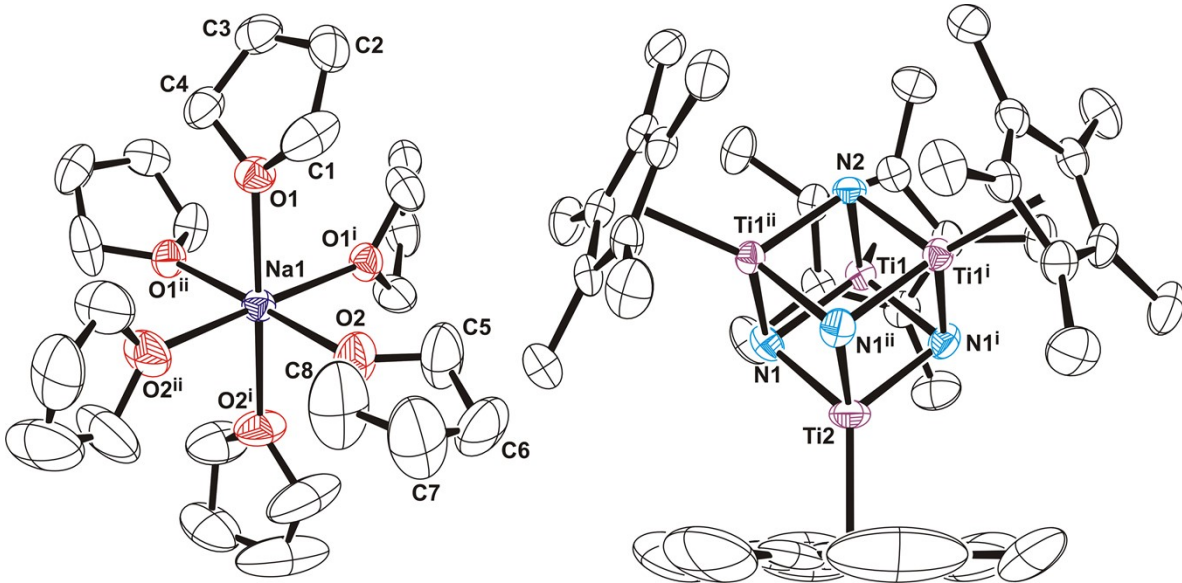


Figure S6. Perspective view of **5** with thermal ellipsoids at the 50% probability level. Hydrogen atoms are omitted for clarity. Symmetry code: (i) z, x, y ; (ii) y, z, x .

Table S2. Selected Lengths (\AA) and Angles (deg) for **5**.

Ti(1)–N(1)	1.954(3)	Ti(1)–N(2)	1.948(3)
Ti(1)–N(1) ⁱ	1.957(3)	Ti(2)–N(1)	1.951(3)
Ti(1)–Ti(2)	2.797(1)	Ti(1)–Ti(1) ⁱ	2.789(1)
Ti(1)–Ti(1) ⁱⁱ	2.789(1)	Na(1)–O(1)	2.395(4)
Na(1)–O(2)	2.360(4)		
N(1)–Ti(1)–N(2)	88.8(1)	N(1)–Ti(1)–N(1) ⁱ	88.4(2)
N(2)–Ti(1)–N(1) ⁱ	88.7(1)	N(1)–Ti(2)–N(1) ⁱ	88.7(1)
Ti(1)–N(1)–Ti(2)	91.5(1)	Ti(1)–N(1)–Ti(1) ⁱⁱ	91.0(1)
Ti(2)–N(1)–Ti(1) ⁱⁱ	91.4(1)	Ti(1)–N(2)–Ti(1) ⁱ	91.4(2)
O(1)–Na(1)–O(2)	90.5(1)	O(1)–Na(1)–O(1) ⁱ	90.9(1)
O(1)–Na(1)–O(2) ⁱ	178.6(2)	O(1)–Na(1)–O(2) ⁱⁱ	89.5(1)
O(2)–Na(1)–O(2) ⁱ	89.1(2)		

Symmetry code: (i) z, x, y ; (ii) y, z, x .

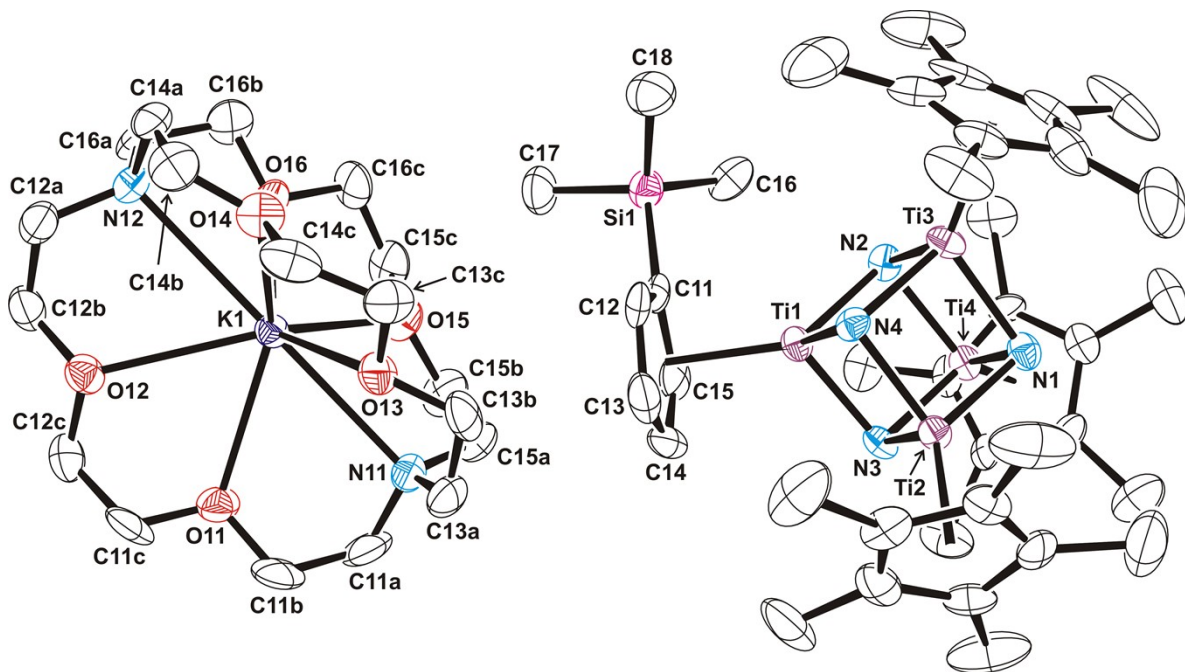


Figure S7. Perspective view of one independent ion pair of **11**·C₆D₆ with thermal ellipsoids at the 50% probability level. Hydrogen atoms and the benzene solvent molecule are omitted for clarity.

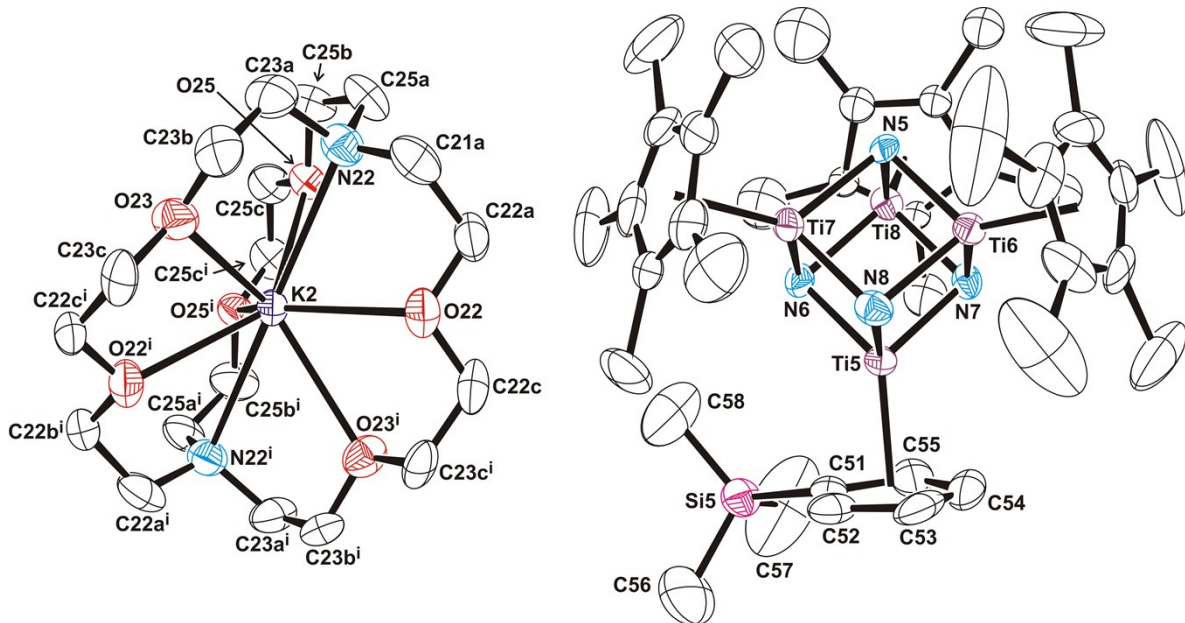


Figure S8. Perspective view of the second independent ion pair of **11**·C₆D₆ with thermal ellipsoids at the 50% probability level. Hydrogen atoms are omitted for clarity. Symmetry code: (i) 2 - x , 1 - y , z .

Table S3. Selected Lengths (Å) and Angles (deg) for **11**·C₆D₆.

Ti(1)–N(2)	1.926(6)	Ti(5)–N(6)	1.913(6)
Ti(1)–N(3)	1.939(6)	Ti(5)–N(7)	1.923(6)
Ti(1)–N(4)	1.945(6)	Ti(5)–N(8)	1.919(6)
Ti(2)–N(1)	1.910(6)	Ti(6)–N(5)	1.922(6)
Ti(2)–N(3)	1.929(6)	Ti(6)–N(7)	1.928(6)
Ti(2)–N(4)	1.953(6)	Ti(6)–N(8)	1.940(6)
Ti(3)–N(1)	1.962(6)	Ti(7)–N(5)	1.959(5)
Ti(3)–N(2)	1.932(6)	Ti(7)–N(6)	1.935(6)
Ti(3)–N(4)	1.937(6)	Ti(7)–N(8)	1.923(6)
Ti(4)–N(1)	1.943(6)	Ti(8)–N(5)	1.927(6)
Ti(4)–N(2)	1.966(6)	Ti(8)–N(6)	1.948(6)
Ti(4)–N(3)	1.904(6)	Ti(8)–N(7)	1.913(6)
Ti(1)–Ti(2)	2.752(2)	Ti(5)–Ti(6)	2.754(2)
Ti(1)–Ti(3)	2.785(2)	Ti(5)–Ti(7)	2.772(2)
Ti(1)–Ti(4)	2.764(2)	Ti(5)–Ti(8)	2.769(2)
Ti(2)–Ti(3)	2.764(2)	Ti(6)–Ti(7)	2.764(2)
Ti(2)–Ti(4)	2.781(2)	Ti(6)–Ti(8)	2.763(2)
Ti(3)–Ti(4)	2.758(2)	Ti(7)–Ti(8)	2.756(2)
K(1)–O	2.785(5)–2.855(5)	K(2)–O	2.806(6)–2.840(5)
K(1)–N	3.004(7)–3.030(6)	K(2)–N(22)	3.015(7)
N–Ti(1)–N av	88.8(9)	N–Ti(5)–N av	88.5(5)
N–Ti–N av	89(1)	N–Ti–N av	88.5(8)
Ti–N(1)–Ti av	91(1)	Ti–N(5)–Ti av	91.0(8)
Ti–N–Ti av	91(1)	Ti–N–Ti av	91.6(7)
O–K(1)–O	59.4(2)–139.2(2)	O–K(2)–O	58.2(2)–137.4(2)
O–K(1)–N	59.6(2)–120.5(2)	O–K(2)–N	60.1(2)–120.1(2)
N–K(1)–N	179.4(2)	N–K(2)–N	179.8(3)

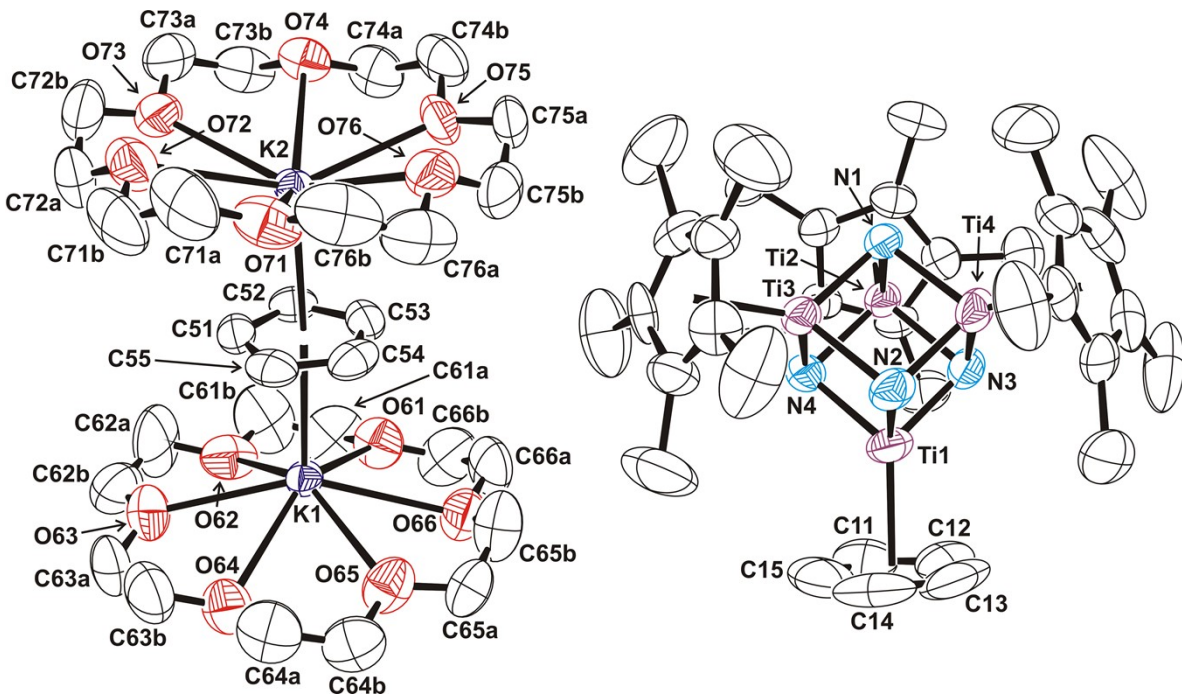


Figure S9. Perspective view of $\mathbf{13} \cdot 2\text{C}_7\text{H}_8$ with thermal ellipsoids at the 50% probability level. Hydrogen atoms are omitted for clarity.

Table S4. Selected Lengths (\AA) and Angles (deg) for $\mathbf{13} \cdot 2\text{C}_7\text{H}_8$.

Ti(1)–N(2)	1.932(4)	Ti(1)–N(3)	1.926(4)
Ti(1)–N(4)	1.926(3)	Ti(2)–N(1)	1.941(3)
Ti(2)–N(3)	1.937(3)	Ti(2)–N(4)	1.941(3)
Ti(3)–N(1)	1.928(3)	Ti(3)–N(2)	1.940(3)
Ti(3)–N(4)	1.933(3)	Ti(4)–N(1)	1.944(3)
Ti(4)–N(2)	1.938(4)	Ti(4)–N(3)	1.935(3)
Ti(1)–Ti(2)	2.771(1)	Ti(1)–Ti(3)	2.769(1)
Ti(1)–Ti(4)	2.769(1)	Ti(2)–Ti(3)	2.777(1)
Ti(2)–Ti(4)	2.764(1)	Ti(3)–Ti(4)	2.770(1)
K(1)–O	2.813(4)–2.957(4)	K(2)–O	2.62(2)–3.05(2)
K(1)–C(ring)	3.058(4)–3.122(4)	K(2)–C(ring)	3.057(4)–3.111(4)
K(1)–Ct	2.856	K(2)–Ct	2.846
N–Ti(1)–N av	88.7(1)	N–Ti–N av	88.5(4)
Ti–N(1)–Ti av	91.2(5)	Ti–N–Ti av	91.5(2)
O–K(1)–O	56.9(1)–150.6(1)	O–K(2)–O	55.8(2)–148.5(1)
K(1)–Ct–K(2)	176.9		

Ct = centroid of the C(51)–C(55) ring.

Table S5. Selected Lengths (\AA) and Angles (deg) for **17**.

K(1)–N(12)	2.904(3)	K(1)–N(13)	3.034(3)
K(1)–N(23)	2.999(3)	K(1)–O(41)	3.085(3)
K(1)–O(42)	2.940(2)	K(1)–O(44)	2.960(2)
K(1)–O(45)	2.862(2)	K(1)–O(46)	2.936(3)
K(1)···O(43)	3.407(3)	Ti(1)–N(12)	1.918(3)
Ti(1)–N(13)	1.886(3)	Ti(2)–N(12)	1.909(3)
Ti(2)–N(23)	1.934(3)	Ti(3)–N(13)	1.882(3)
Ti(3)–N(23)	1.941(3)	Ti(1)–N(1)	1.951(3)
Ti(2)–N(1)	1.922(3)	Ti(3)–N(1)	1.927(3)
K(1)···Ti(1)	3.657(1)	K(1)···Ti(2)	3.691(1)
K(1)···Ti(3)	3.762(1)	Ti(1)···Ti(2)	2.787(1)
Ti(1)···Ti(3)	2.768(1)	Ti(2)···Ti(3)	2.800(1)
N(12)–K(1)–N(13)	61.1(1)	N(12)–K(1)–N(23)	61.2(1)
N(13)–K(1)–N(23)	59.8(1)	O(41)–K(1)–O(42)	56.2(1)
O(41)–K(1)–O(44)	117.6(1)	O(41)–K(1)–O(45)	98.5(1)
O(41)–K(1)–O(46)	50.2(1)	O(42)–K(1)–O(44)	98.0(1)
O(42)–K(1)–O(45)	133.6(1)	O(42)–K(1)–O(46)	106.1(1)
O(44)–K(1)–O(45)	56.9(1)	O(44)–K(1)–O(46)	109.0(1)
O(45)–K(1)–O(46)	58.4(1)	N(12)–K(1)–O(41)	96.6(1)
N(12)–K(1)–O(42)	80.9(1)	N(12)–K(1)–O(44)	138.1(1)
N(12)–K(1)–O(45)	144.6(1)	N(12)–K(1)–O(46)	111.4(1)
N(13)–K(1)–O(41)	113.5(1)	N(13)–K(1)–O(42)	140.0(1)
N(13)–K(1)–O(44)	118.0(1)	N(13)–K(1)–O(45)	83.6(1)
N(13)–K(1)–O(46)	79.3(1)	N(23)–K(1)–O(41)	157.6(1)
N(23)–K(1)–O(42)	113.4(1)	N(23)–K(1)–O(44)	81.9(1)
N(23)–K(1)–O(45)	101.6(1)	N(23)–K(1)–O(46)	137.1(1)
N(12)–Ti(1)–N(13)	105.0(1)	N(12)–Ti(2)–N(23)	102.9(1)
N(13)–Ti(3)–N(23)	103.8(1)	N(1)–Ti(1)–N(12)	86.4(1)
N(1)–Ti(1)–N(13)	86.5(1)	N(1)–Ti(2)–N(12)	87.4(1)
N(1)–Ti(2)–N(23)	87.0(1)	N(1)–Ti(3)–N(13)	87.3(1)
N(1)–Ti(3)–N(23)	86.6(1)	K(1)–N(12)–Ti(1)	96.5(1)
K(1)–N(12)–Ti(2)	98.0(1)	Ti(1)–N(12)–Ti(2)	93.5(1)
K(1)–N(13)–Ti(1)	93.1(1)	K(1)–N(13)–Ti(3)	97.1(1)
Ti(1)–N(13)–Ti(3)	94.5(1)	K(1)–N(23)–Ti(2)	94.4(1)
K(1)–N(23)–Ti(3)	96.8(1)	Ti(2)–N(23)–Ti(3)	92.5(1)
Ti(1)–N(1)–Ti(2)	92.0(1)	Ti(1)–N(1)–Ti(3)	91.1(1)
Ti(2)–N(1)–Ti(3)	93.3(1)		

EPR spectroscopy

A 5 mM frozen pyridine solution of compound **7** was registered in a Bruker Magnettech ESR5000 spectrometer.

Experimental parameters:

Temperature = 93 K; MW power = 2.51 mW; modulation frequency = 100 kHz;
modulation = 0.05 mT.

Simulation parameters were performed using the EasySpin toolbox in Matlab (S. Stoll and A. Schweiger, *J. Magn. Reson.* 2006, **178**, 42–55):

Compound **7**: $g = [1.996]$; $\text{lwpp} = [1,963 \ 1,697]$

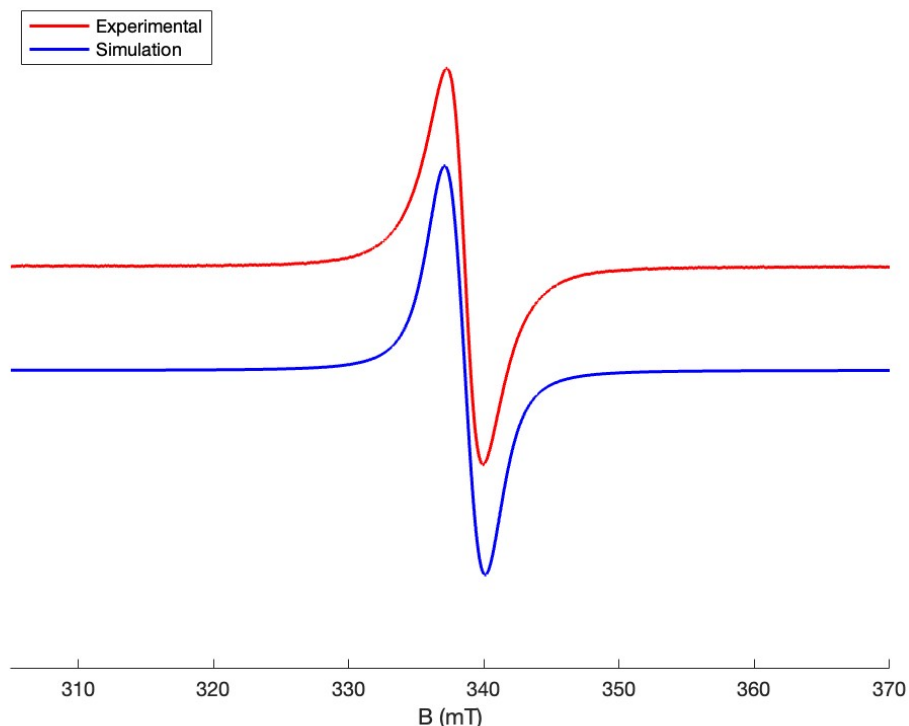


Figure S10. Low-temperature (93 K) EPR spectra of **7** ($g = 1.996$).

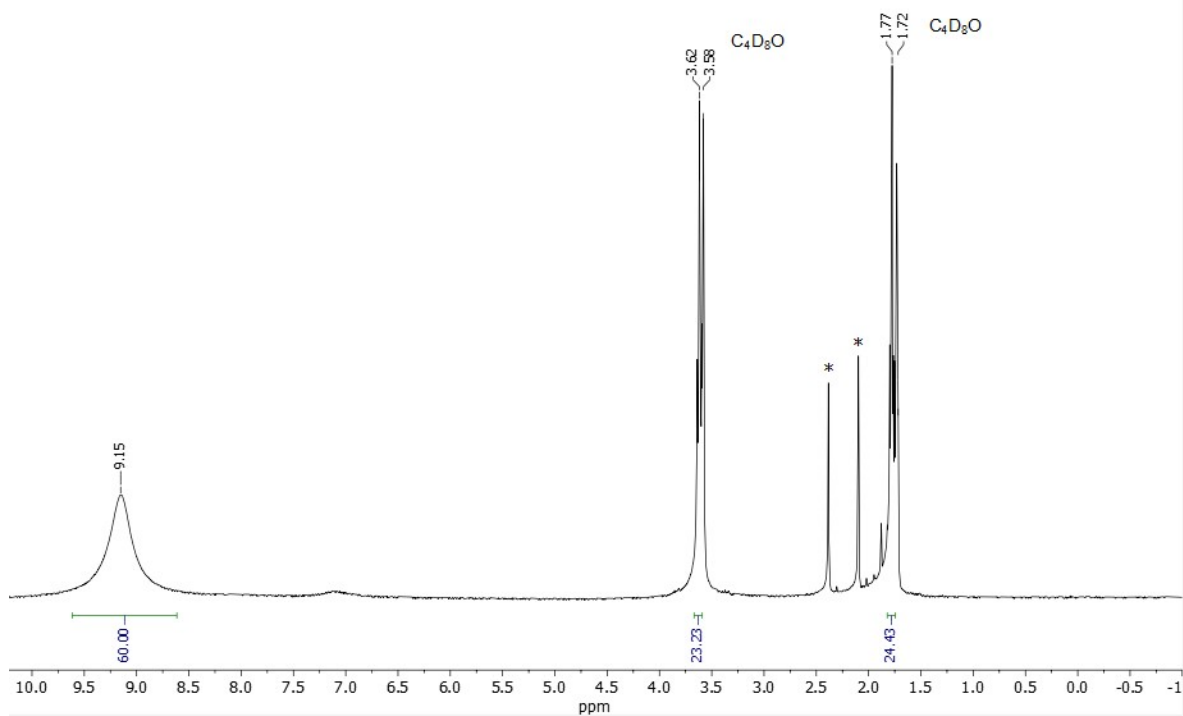


Figure S11. ^1H NMR spectrum (300 MHz, $\text{C}_4\text{D}_8\text{O}$, 20 °C) of $[\text{Na}(\text{thf})_6][\{\text{Ti}(\eta^5\text{-C}_5\text{Me}_5)\}_4(\mu_3\text{-N})_4]$ (**5**). *Unknown species.

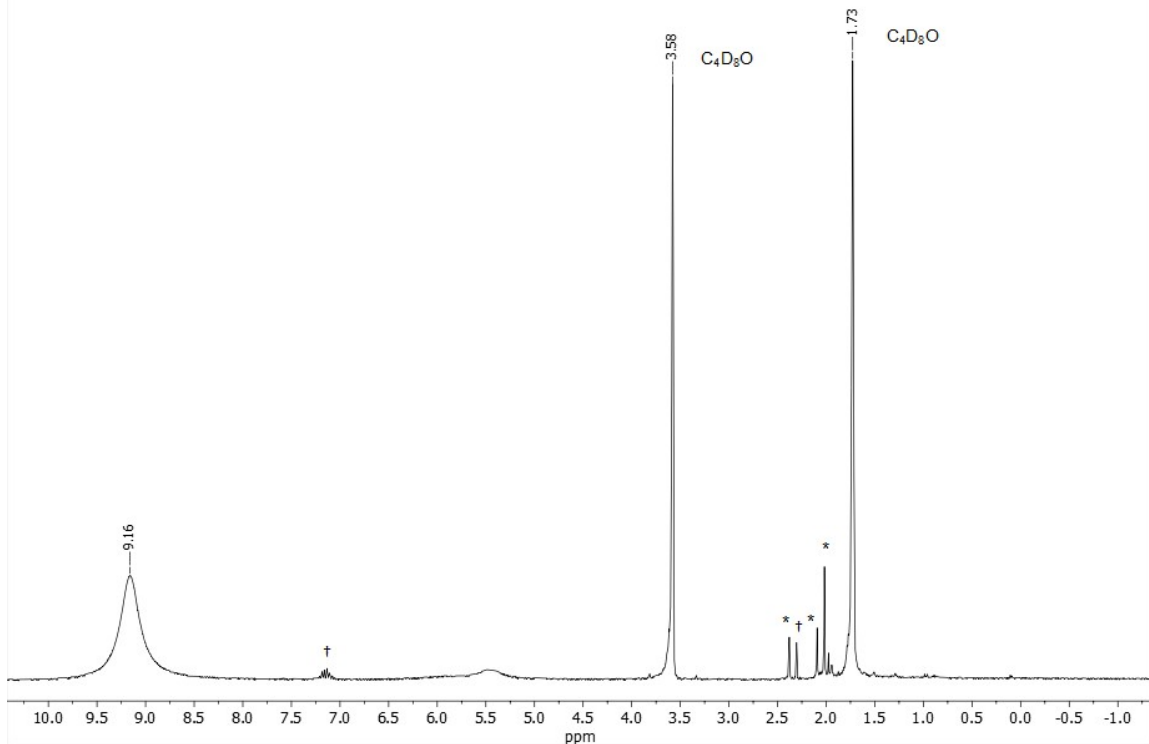


Figure S12. ^1H NMR spectrum (300 MHz, $\text{C}_4\text{D}_8\text{O}$, 20 °C) of $\text{Na}[\{\text{Ti}(\eta^5\text{-C}_5\text{Me}_5)\}_4(\mu_3\text{-N})_4]$. *Unknown species. †Toluene.

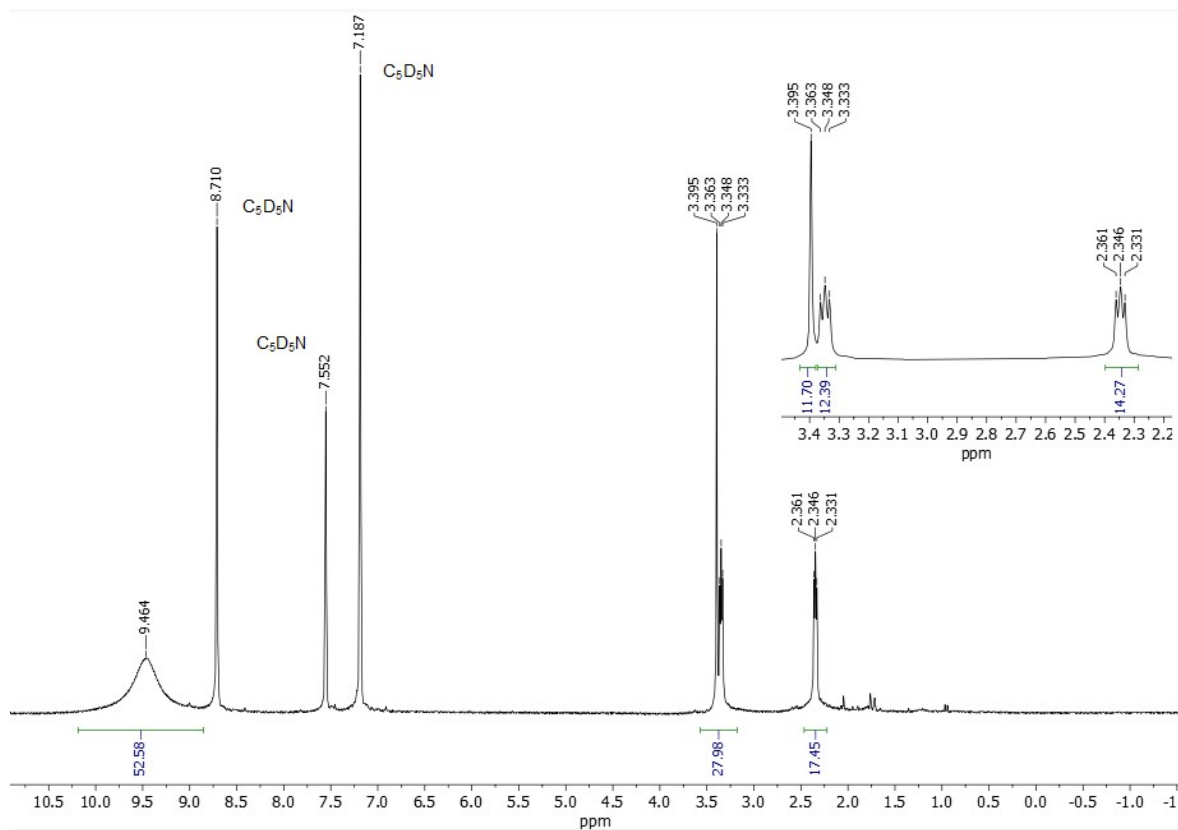


Figure S13. ¹H NMR spectrum (300 MHz, C₅D₅N, 20 °C) of [K(crypt-222)][{Ti(η⁵-C₅Me₅)₄(μ₃-N)₄}] (7).

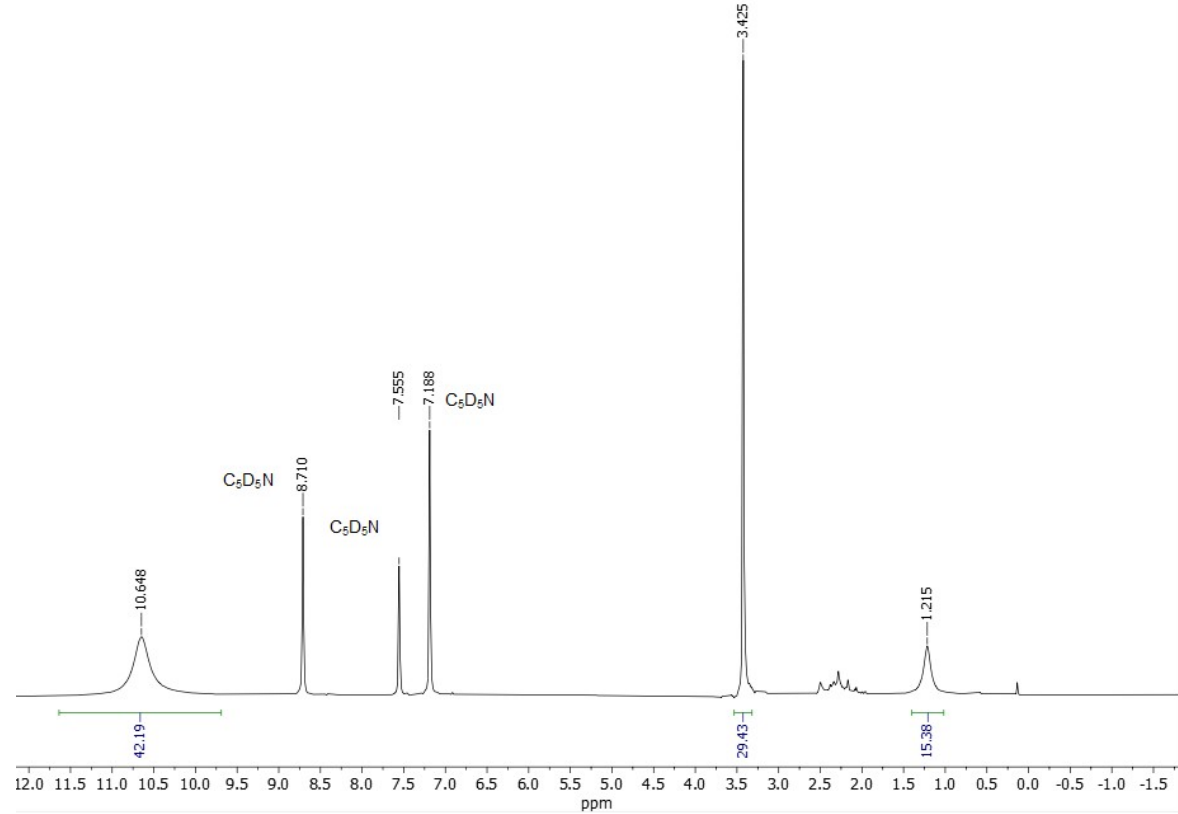


Figure S14. ¹H NMR spectrum (300 MHz, C₅D₅N, 20 °C) of [K(18-crown-6)][(Ti₄(η⁵-C₅Me₅)₃{N(SiMe₃)₂})(μ₃-N)₄] (8).

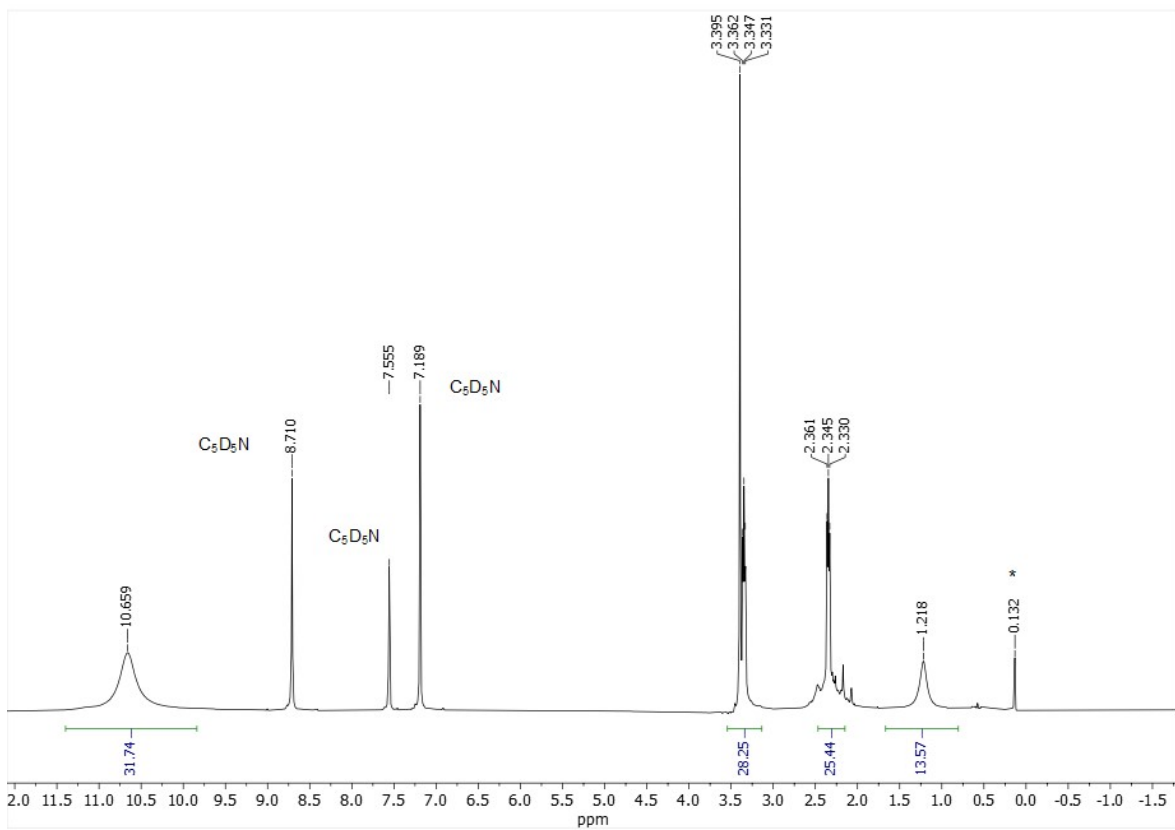


Figure S15. ^1H NMR spectrum (300 MHz, $\text{C}_5\text{D}_5\text{N}$, 20 °C) of $[\text{K}(\text{crypt-222})][(\text{Ti}_4(\eta^5\text{-C}_5\text{Me}_5)_3\{\text{N}(\text{SiMe}_3)_2\})(\mu_3\text{-N})_4]$ (**9**). *Silicone grease.

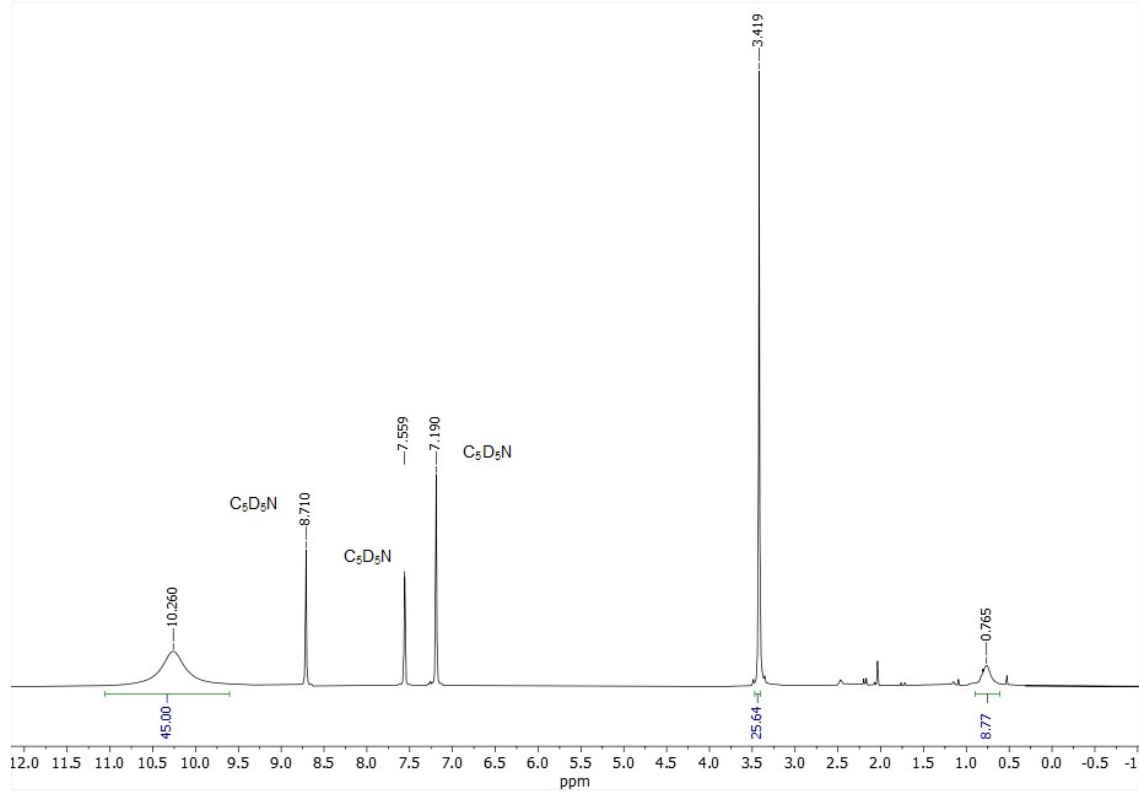


Figure S16. ^1H NMR spectrum (300 MHz, $\text{C}_5\text{D}_5\text{N}$, 20 °C) of $[\text{K}(18\text{-crown-6})][\{\text{Ti}_4(\eta^5\text{-C}_5\text{Me}_5)_3(\eta^5\text{-C}_5\text{H}_4\text{SiMe}_3)\}(\mu_3\text{-N})_4]$ (**10**).

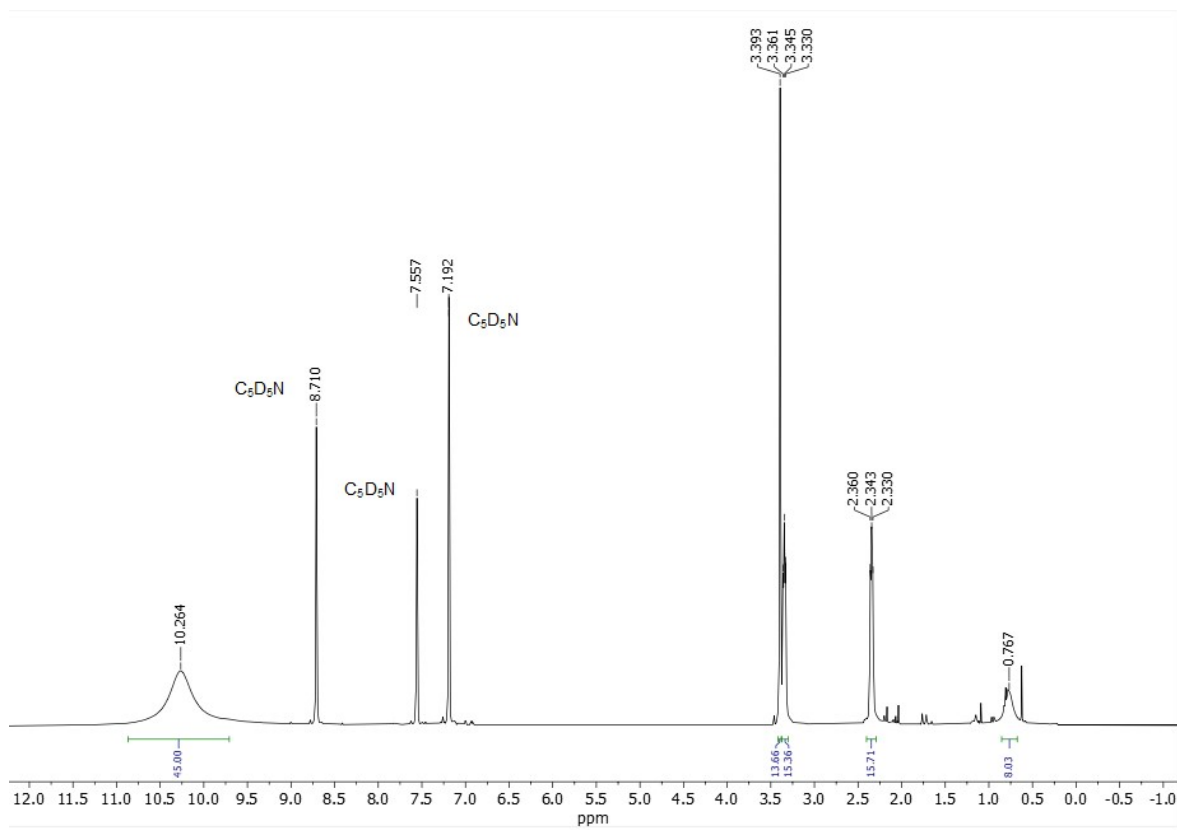


Figure S17. ¹H NMR spectrum (300 MHz, C_5D_5N , 20 °C) of $[K(\text{crypt-222})][\{\text{Ti}_4(\eta^5\text{-C}_5\text{Me}_5)_3(\eta^5\text{-C}_5\text{H}_4\text{SiMe}_3)\}(\mu_3\text{-N})_4]$ (**11**).

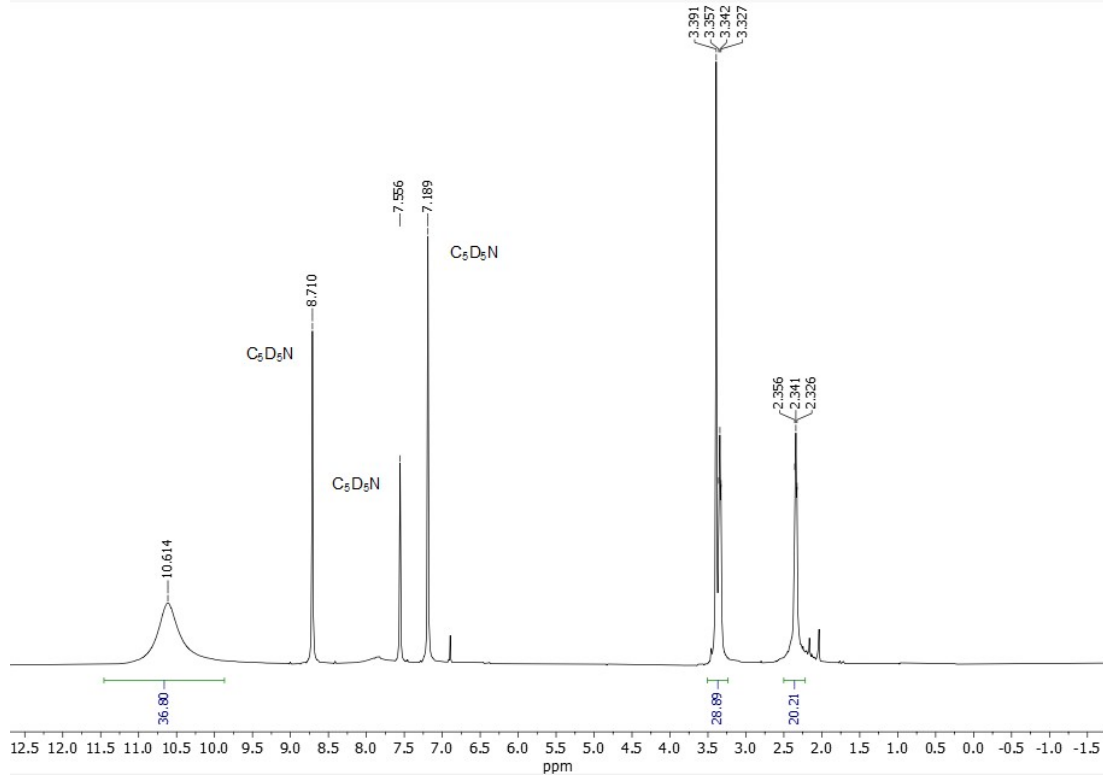
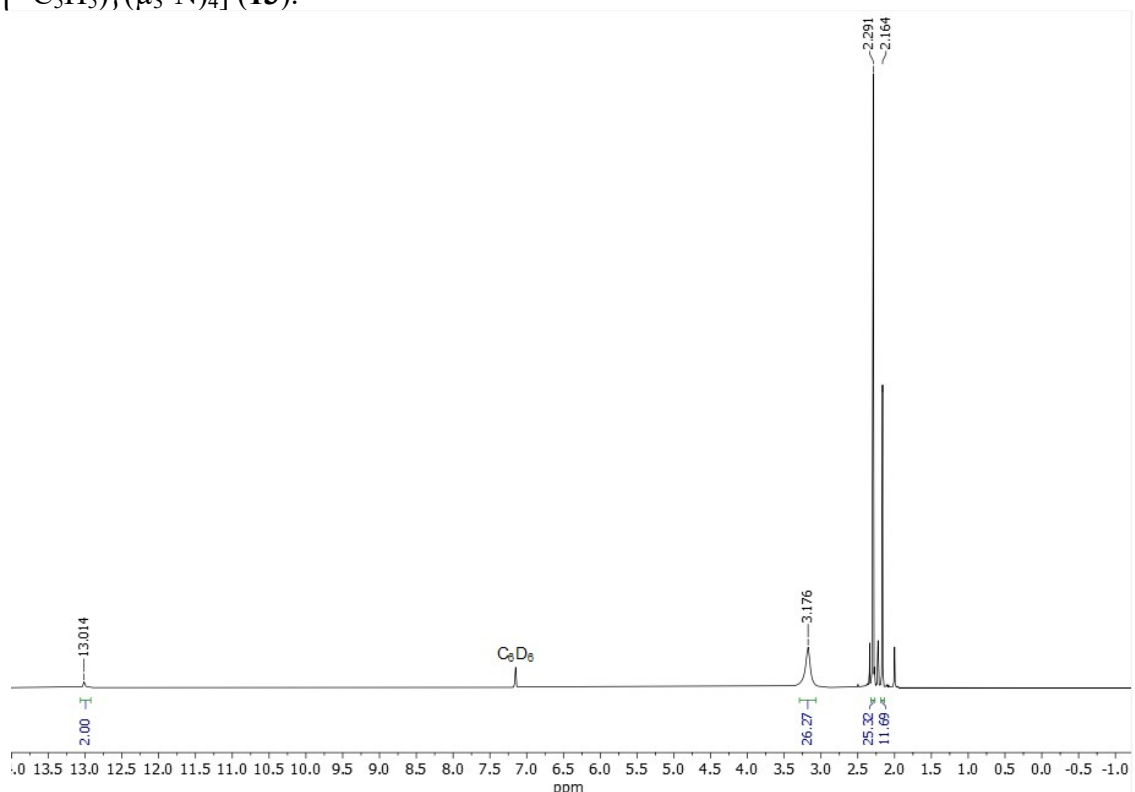
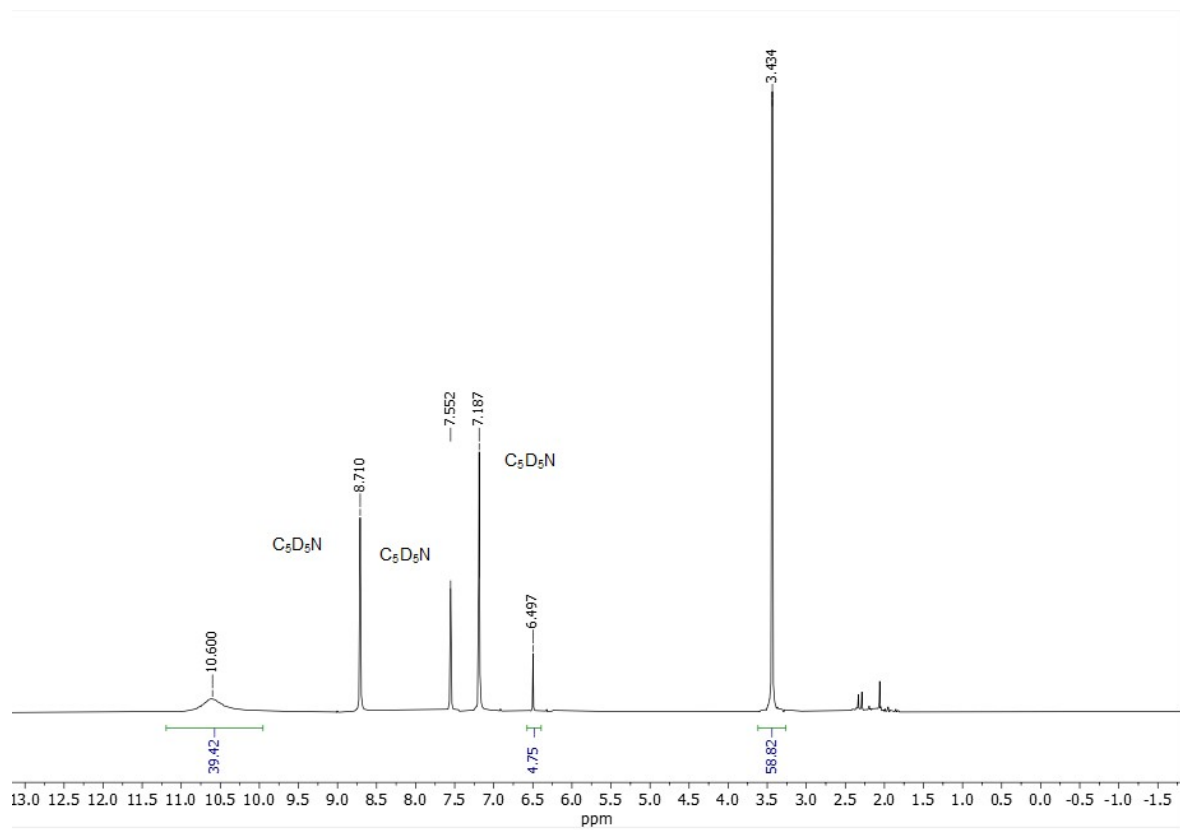


Figure S18. ¹H NMR spectrum (300 MHz, C_5D_5N , 20 °C) of $[K(\text{crypt-222})][\{\text{Ti}_4(\eta^5\text{-C}_5\text{Me}_5)_3(\eta^5\text{-C}_5\text{H}_5)\}(\mu_3\text{-N})_4]$ (**12**).



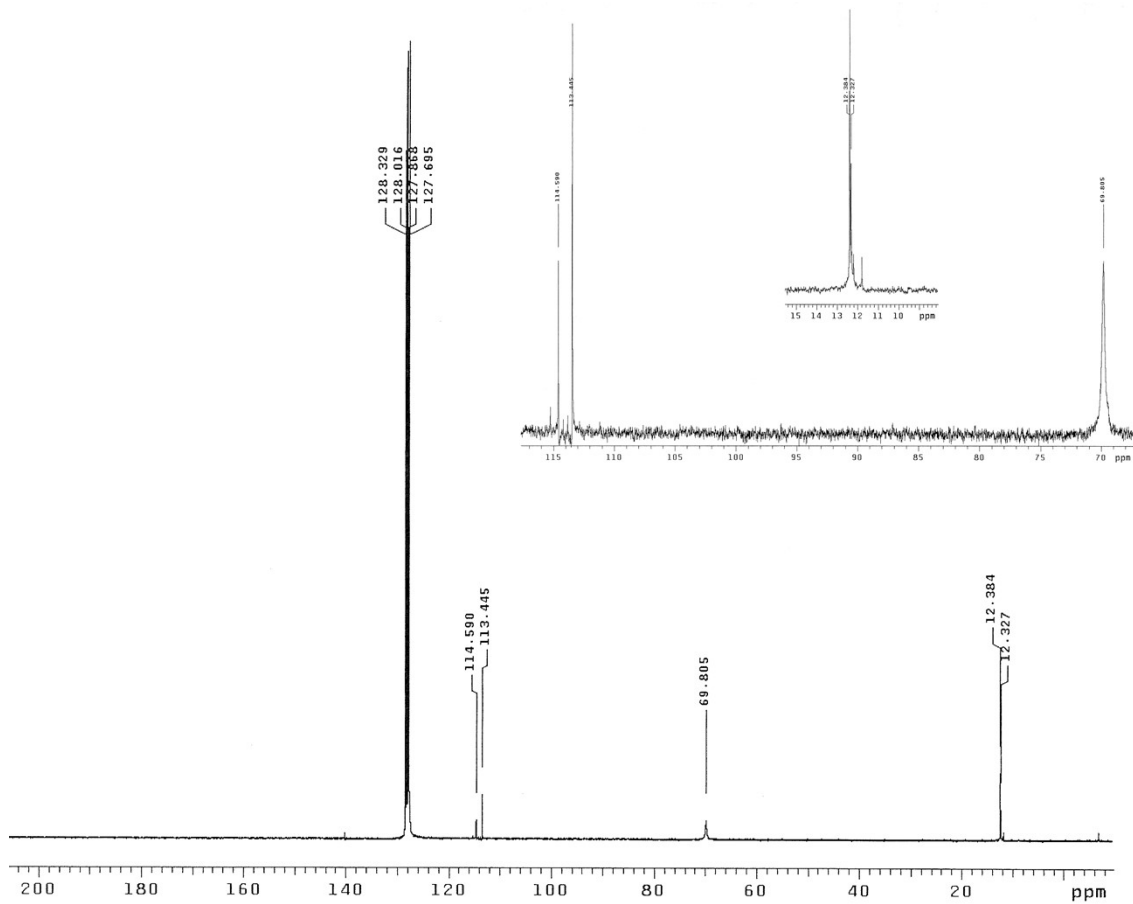


Figure S21. $^{13}\text{C}\{\text{H}\}$ NMR spectrum (75 MHz, C_6D_6 , 20 °C) of $[(18\text{-crown-6})\text{K}\{(\mu_3\text{-N})(\mu_3\text{-NH})_2\text{Ti}_3(\eta^5\text{-C}_5\text{Me}_5)_3(\mu_3\text{-N})\}]$ (**16**).

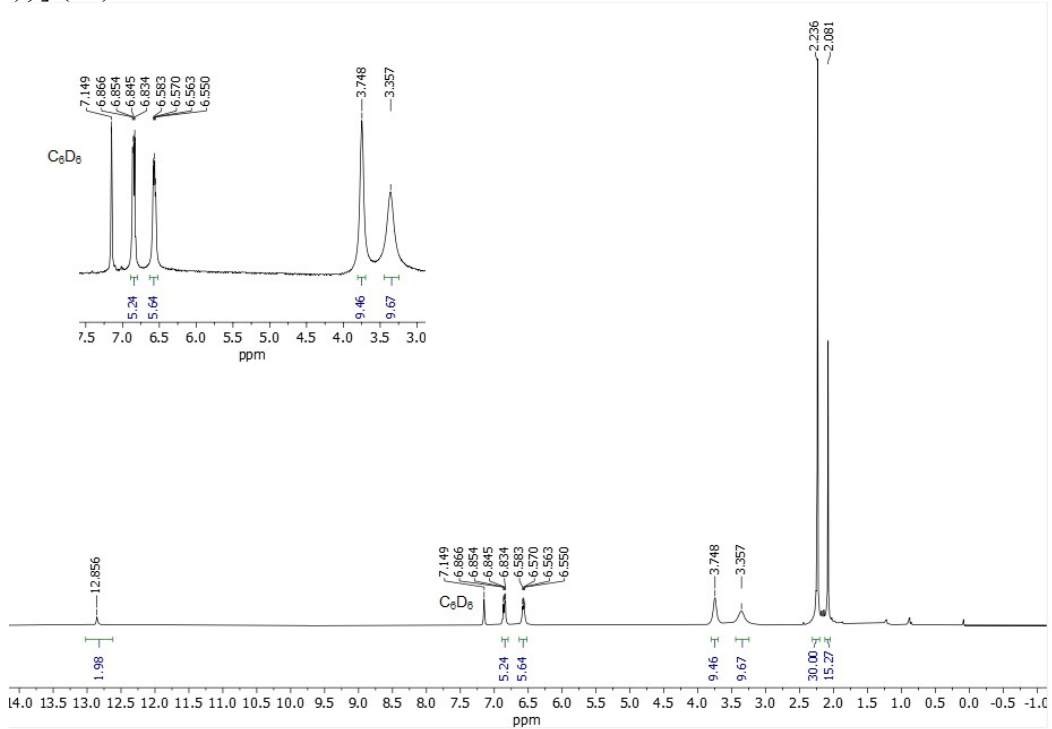


Figure S22. ^1H NMR spectrum (300 MHz, C_6D_6 , 20 °C) of $[(\text{dibenzo-18-crown-6})\text{K}\{(\mu_3\text{-N})(\mu_3\text{-NH})_2\text{Ti}_3(\eta^5\text{-C}_5\text{Me}_5)_3(\mu_3\text{-N})\}]$ (**17**).

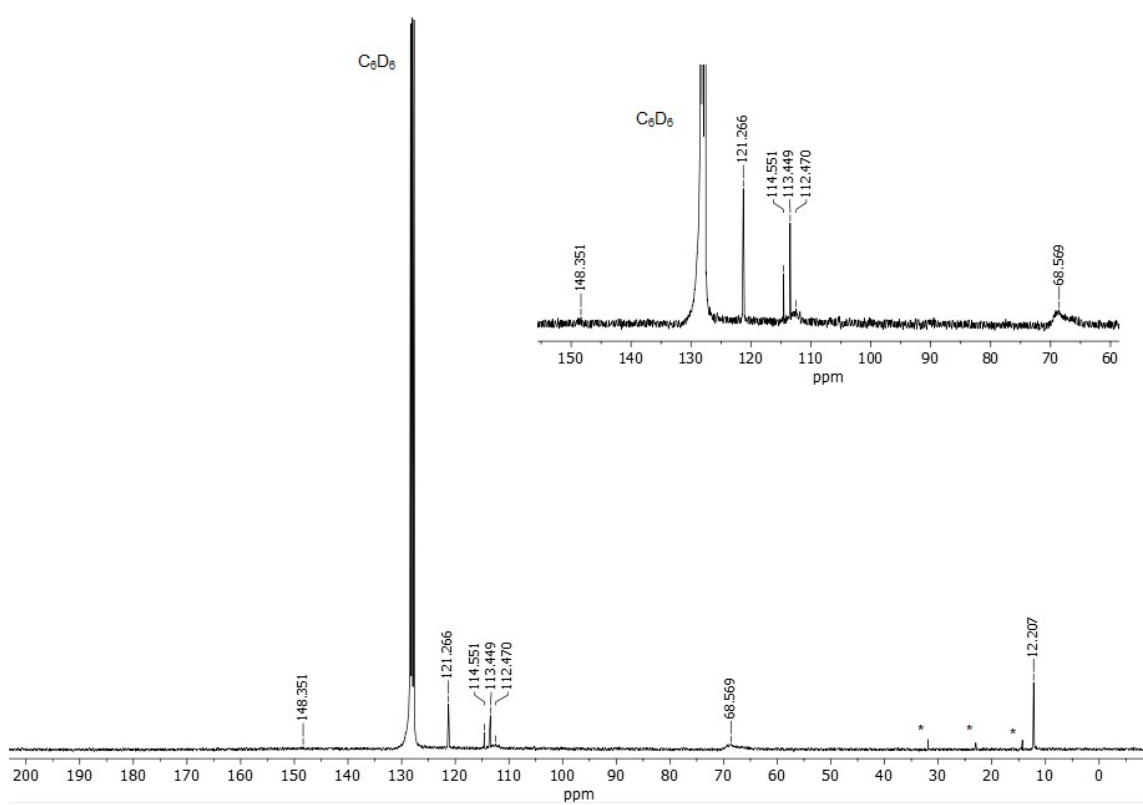


Figure S23. $^{13}\text{C}\{^1\text{H}\}$ NMR spectrum (75 MHz, C_6D_6 , 20 °C) of $[(\text{dibenzo-18-crown-6})\text{K}\{(\mu_3\text{-N})(\mu_3\text{-NH})_2\text{Ti}_3(\eta^5\text{-C}_5\text{Me}_5)_3(\mu_3\text{-N})\}]$ (**17**). * n -hexane.

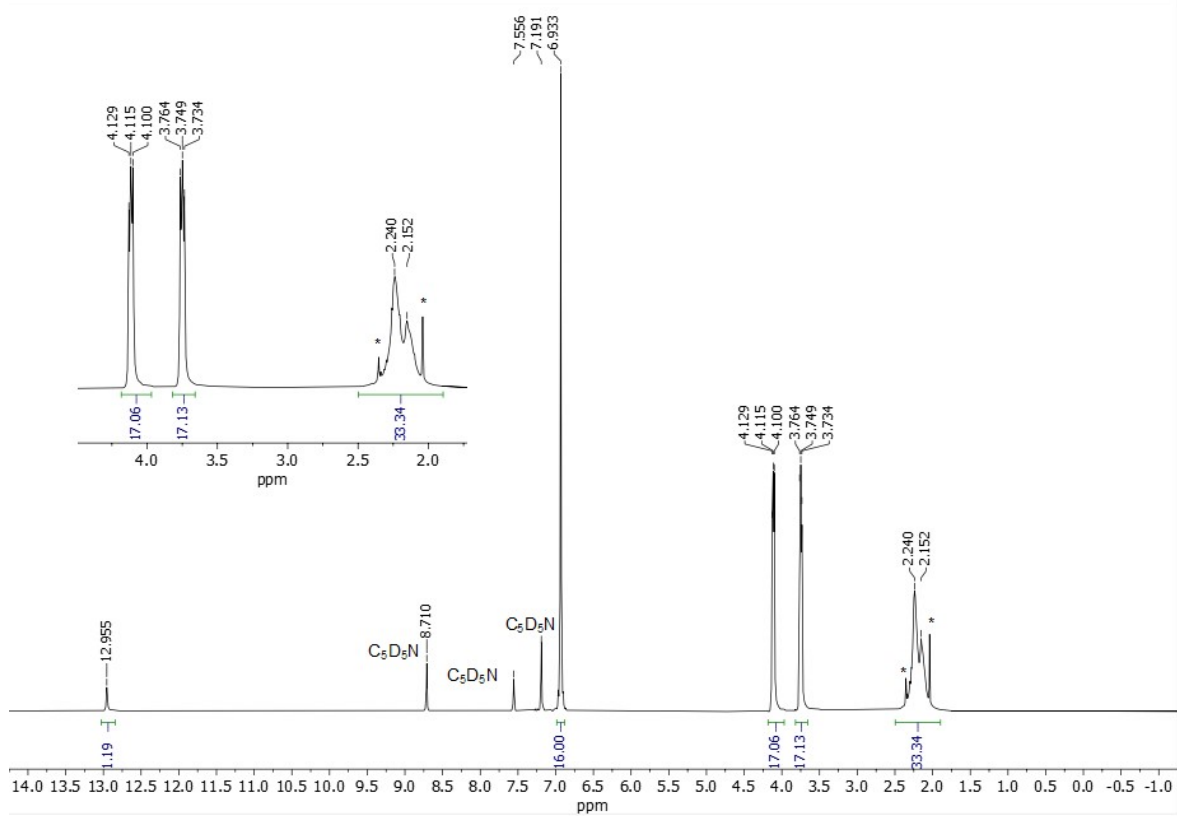


Figure S24. ^1H NMR spectrum (300 MHz, $\text{C}_6\text{D}_5\text{N}$, 20 °C) of $[\text{K}(\text{dibenzo-18-crown-6})_2][\text{Ti}_3(\eta^5\text{-C}_5\text{Me}_5)_3(\mu_3\text{-N})(\mu\text{-NH})_2]$ (**18**). *Unknown species.

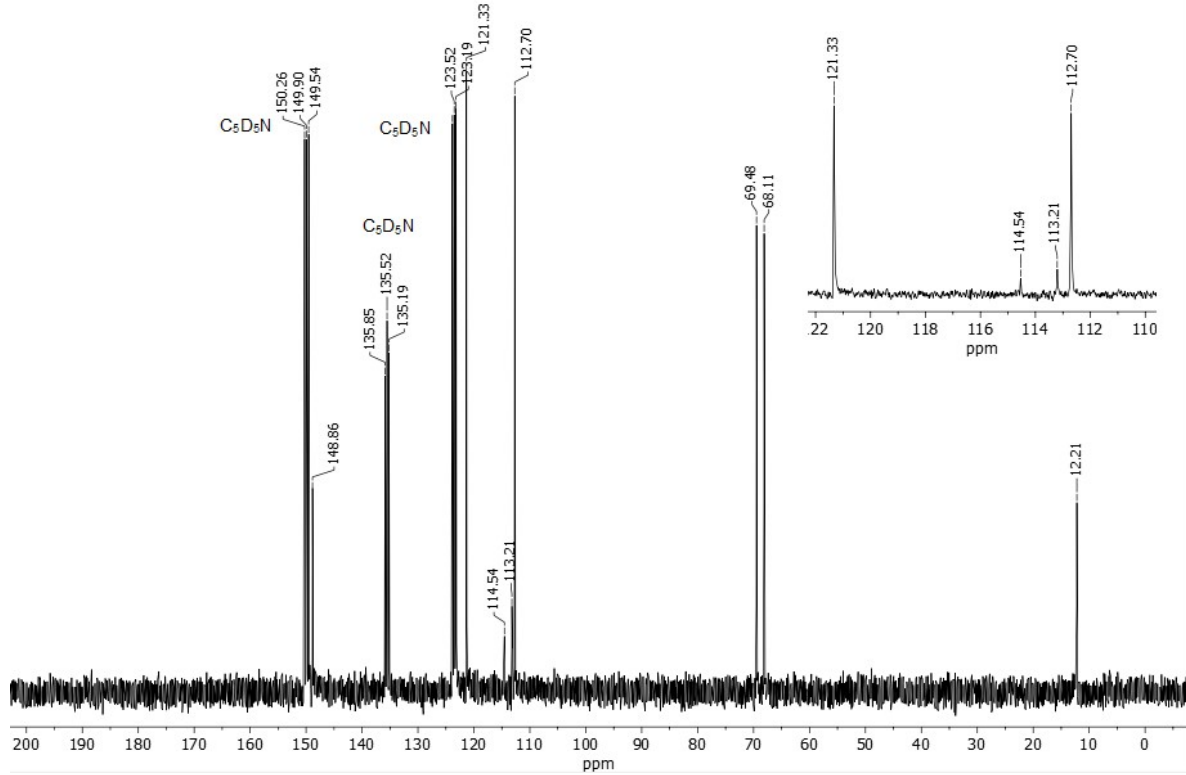


Figure S25. $^{13}\text{C}\{\text{H}\}$ NMR spectrum (75 MHz, $\text{C}_5\text{D}_5\text{N}$, 20 °C) of $[\text{K}(\text{dibenzo-18-crown-6})_2]\text{[Ti}_3(\eta^5\text{-C}_5\text{Me}_5)_3(\mu_3\text{-N})(\mu\text{-NH})_2]$ (**18**).

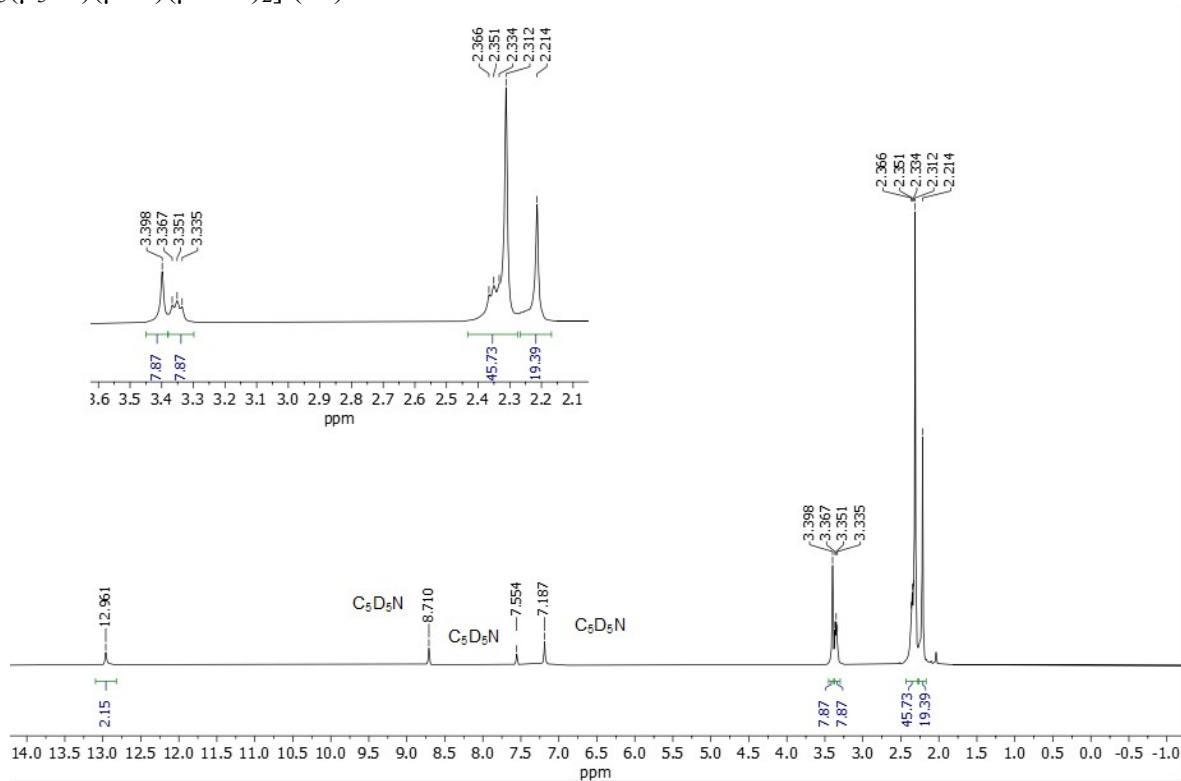


Figure S26. ^1H NMR spectrum (300 MHz, $\text{C}_5\text{D}_5\text{N}$, 20 °C) of $[\text{K}(\text{crypt-222})]\text{[Ti}_3(\eta^5\text{-C}_5\text{Me}_5)_3(\mu_3\text{-N})(\mu\text{-N})(\mu\text{-NH})_2]$ (**19**).

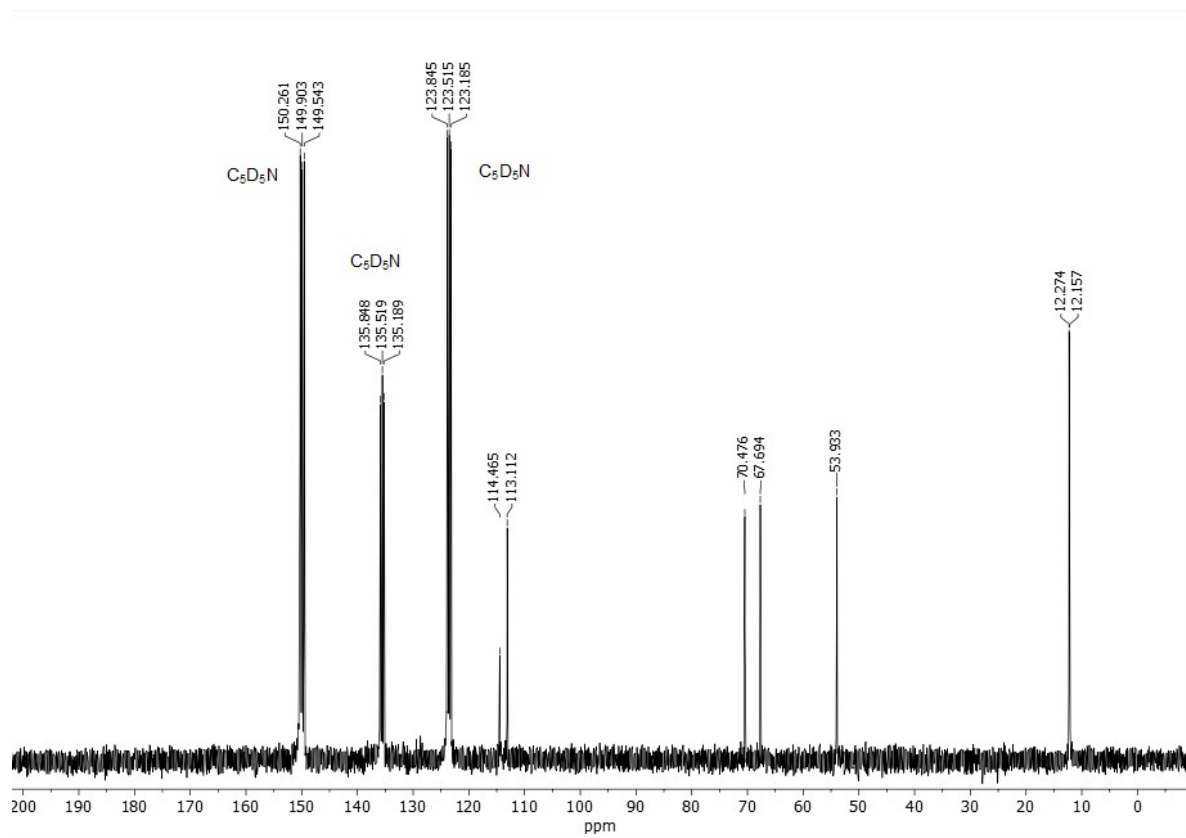


Figure S27. $^{13}\text{C}\{\text{H}\}$ NMR spectrum (75 MHz, $\text{C}_5\text{D}_5\text{N}$, 20 °C) of $[\text{K}(\text{crypt}-222)][\text{Ti}_3(\eta^5-\text{C}_5\text{Me}_5)_3(\mu_3-\text{N})(\mu-\text{N})(\mu-\text{NH})_2]$ (**19**).